Tooeleite Transformation and Coupled As(III) Mobilization Are Induced by Fe(II) under Anoxic, Circumneutral Conditions

Girish Choppala,* Dane Lamb, Robert Aughterson, and Edward D. Burton

ACCESS | Metrics & More | Article Recommendations | SI Supporting Information

ABSTRACT: Tooeleite $[Fe^{III}_6(As^{III}O_3)_4SO_4(OH)_4.4H_2O]$ is an important As(III) host phase in diverse mining-impacted environments. Tooeleite has also received attention as a target phase for immobilizing As(III) in environmental and engineered settings. However, little is known regarding tooeleite's environmental stability, with no previous research examining the possible role of Fe(II) in inducing tooeleite transformation (as occurs for Fe(III) oxide minerals). We investigated shifts in solid-phase Fe and As speciation and associated As mobilization into the aqueous phase during exposure of tooeleite to aqueous Fe(II) under anoxic conditions at pH 4 to 8. Our results demonstrate that environmentally relevant concentrations of aqueous Fe(II) (i.e., 1 to 10 mM) induce significant mobilization of As(III) from tooeleite under near-neutral pH conditions, with greater As(III) mobilization occurring at higher pH. Extended X-ray absorption fine structure spectroscopy at both the As and Fe K-edge reveals that the observed As(III) mobilization was coupled with partial Fe(II)-induced transformation of tooeleite to As(III)-bearing ferrihydrite at pH 6 to 8. These results provide new insights into the environmental stability of tooeleite and demonstrate a novel pathway for As(III) mobilization in tooeleite-bearing systems.

KEYWORDS: arsenic, contamination, mine sites, ferrihydrite, X-ray absorption spectroscopy
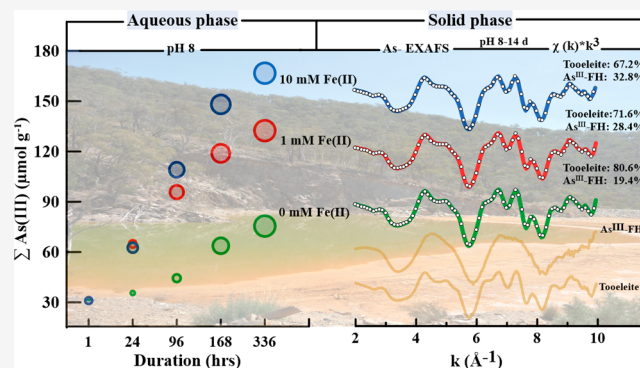
INTRODUCTION

Arsenic (As) is a ubiquitous toxin that poses a significant global environmental and public health challenge.[1−3] Elevated levels of As have been documented in water resources worldwide, with particularly severe As contamination arising from mining of sulfide ores.[4−6] Arsenic contamination is a well-recognized environmental issue that is associated with many former mine sites.[7−10]

The toxicity and environmental mobility of As is controlled by myriad geochemical reactions, depending on chemical speciation and mineralogy.[11,12] In general, As typically exists in most near-surface environments as the oxygen-coordinated arsenite [As(III)] and arsenate [As(V)] species. Arsenite is thought to be 25−60 times as toxic and more soluble and environmentally mobile than As(V).[13,14] Thus, resolving the stability and potential transformation of As(III) bearing minerals is crucial to understanding the environmental cycling of As.[15]

Tooeleite $[Fe_6(AsO_3)_4SO_4(OH)_4.4H_2O]$ is the only known As(III)-Fe(III) mineral.[16] It accumulates in acidic systems that are rich in As(III), iron, and sulfate. Tooeleite can be considered to be an example of an anthropogenic mineral, in that it originates as a result of human activities (i.e., mining or mineral processing). As such, tooeleite has been reported to

occur in As(III)-rich acid mine drainage (AMD),[17−19] mining waste-rock and tailings,[20−23] hydrometallurgical waste,[21] and surface soils of mine sites.[24] Understanding tooeleite formation, stability, and fate is of increasing interest from the perspective of managing As mobility in mining-impacted systems.[25,26]

Many abandoned mine sites and associated mining-impacted systems contain As-contaminated waste and soil that experience periodical waterlogging, which can lead to partial reductive dissolution of Fe(III)-bearing minerals.[27,28] The resulting juxtaposition of newly produced aqueous Fe(II) and residual Fe(III)-bearing minerals may lead to rapid Fe(II)-induced mineral transformation and/or recrystallization processes.[28−31] Previous research examining Fe(III) oxides, such as ferrihydrite and schwertmannite, has shown that Fe(II)-induced transformation can have substantial effects on the speciation and mobility of co-associated As.[32−35]

To date, there is significant uncertainty regarding tooeleite's environmental stability. It appears that, under oxic conditions, tooeleite may transform to a series of Fe-As phases, including scorodite (Fe(III)-As(V) oxide) as well as jarosite, schwertmannite, and ferrihydrite, where the newly formed Fe(III) phases can retain As(III) and As(V) through adsorption and coprecipitation processes.[36] However, we currently have little information on tooeleite's environmental behavior under anoxic conditions (e.g., in waterlogged soil or mine waste). In particular, no previous studies have examined if Fe(II) can induce the transformation of tooeleite, thereby potentially leading to As(III) mobilization.

Therefore, the objective of the present study was to investigate the fate of As and Fe following the exposure of tooeleite to a range of environmentally relevant Fe(II) concentrations and pH conditions. Accordingly, we use X-ray absorption spectroscopy (XAS), transmission electron microscopy (TEM), and X-ray diffraction (XRD) to characterize solid-phase As and Fe behavior, while also monitoring aqueous phase As speciation during the exposure of tooeleite to up to 10 mM aqueous Fe(II) over 14 days at pH 4−8.

■ EXPERIMENTAL DESIGN

Chemicals and Reagents. Chemical reagents were sourced from Sigma-Aldrich (Australia). Experimental solutions were prepared by using Type I water (18.2 MΩ cm). All glassware was acid-washed for at least 12 h and rinsed with Type I water. Experiments were performed in triplicate at ambient temperature (22 °C). Oxygen-free conditions were maintained throughout experimental work using an anaerobic chamber containing an atmosphere of 97−98% N_2 and 2−3% H_2.

Synthesis of Tooeleite. Tooeleite was synthesized as described by Li et al.[36] The synthesis procedure involved the addition of 0.14 M As(III) solution (adjusting the pH to 1.3 by H_2SO_4) with 1 L equiv molar concentration of Fe(III) solution in a constant-temperature glass beaker. The resulting suspension was agitated for 2 h at 95 °C at 50 rpm, while pH was maintained at pH 2 by the slow addition of 1 M NaOH. The suspension was then cooled to room temperature, washed five times with deionized water, dried in a fan-forced oven at 80 °C, ground to a fine powder using a stainless-steel mechanical ball mill, and stored in a glass container for use in subsequent experiments. We acknowledge that drying of tooeleite may result in aggregation behavior that contrasts with corresponding freshly prepared tooeleite that is maintained as an aqueous suspension. However, it should be noted that tooeleite has been observed in relatively dry material at several field sites,[20,24] and it is therefore reasonable to assume that drying of synthetic tooeleite likely induces a similar degree aggregation as that occurs for natural tooeleite exposed to dry conditions in mine wastes or mine-site soils.

Transformation Experiment. Experimental examination of the impact of Fe(II) on tooeleite behavior and As mobility followed a general procedure for examining Fe(II)-induced Fe(III) mineral transformation as described by Choppala and Burton.[30] Synthetic tooeleite (0.2 g) was pre-equilibrated for 24 h in 40 mL of deoxygenated 0.1 M KCl background solution that was adjusted to pH 4, 6, or 8 (noncomplexing tertiary amine buffers, PIPPS, and MES at 0.05 M, were used to maintain the desired pH). Following pre-equilibration, 1 M Fe(II) stock solution (prepared from $FeCl_2 \cdot 4H_2O$, Sigma-Aldrich) was added to achieve a final Fe(II) concentration of 0,

1, and 10 mM. Triplicate subsamples of each treatment were sacrificed at predetermined time intervals and centrifuged (4000 rpm), and the supernatant was filtered to <0.22 μm and acidified to pH < 2 using HCl. At each sampling time, solid-phase samples were subsequently rinsed with N_2-purged methanol and dried within an anaerobic chamber to prevent further mineralogical transformation.

Analyses. Concentrations of aqueous As(III) and As(V) were measured by high-performance liquid chromatography (Agilent 1100, Agilent Technologies, Japan, equipped with a guard column and a Hamilton PRP-X100 separation column) coupled to an inductively coupled plasma-mass spectrometry (HPLC-ICP-MS), with a detection limit of <0.3 μg L^{-1} (Agilent 7900, Agilent Technologies, Tokyo, Japan).[37]

Mineralogy was evaluated by powder XRD (Malvern PANalytical Empyrean, UK). Ground powdered samples were homogenized and mounted on low background quartz sample holders in an anaerobic glovebox to avoid oxidation artifacts. The diffraction patterns were recorded in continuous scan mode with 2θ angles from 5 to 80° with a step size of 0.02° 2θ and 1 s counting time per step. The XRD patterns were evaluated using the X'Pert High Score Plus diffraction software (Malvern PANalytical, Malvern, UK).

The solid-phase micromorphology of individual particles was examined using scanning electron microscopy with energy-dispersive X-ray spectroscopy (SEM−EDX, Zeiss EVOLS-15, Germany). In addition, the spatial distribution of As and Fe and the crystal morphology in secondary mineral products were examined using a JEOL JEM-2200FS transmission electron microscope (TEM) at the Australian Nuclear Science and Technology Organization (Sydney, Australia). Selected experimental samples for TEM examination were suspended in absolute ethanol and disaggregated by grinding using a mortar and pestle. A drop of suspension was placed onto a Cu grid with a lacy-carbon support, and then immediately loaded into a JEOL double-tilt, analytical specimen holder. Observations of individual mineral particles were undertaken at a voltage of 200 kV. Analyses was performed using *Digital Micrograph* (Gatan Inc. USA) to measure *d*-spacings from selected areas.

Arsenic K-edge XAS data were collected in fluorescence mode, using a Si(111) double crystal monochromator, at approximately 5 K in a He atmosphere with the use of a 100-element solid-state HP-Ge detector (Canberra/Mirion, France) at the Australian Synchrotron. Self-absorption was minimized by diluting the samples and reference standards to ∼0.1 wt % As with cellulose. Quantification of the relative abundances of solid-phase As(III) and As(V) was determined by linear combination fitting (LCF) of X-ray absorption near edge structure (XANES) spectra against As(III) and As(V) reference standards (i.e., $NaAsO_2$ and Na_3AsO_4, respectively). Solid-phase As speciation was further evaluated by fitting of k^3-weighted extended X-ray absorption fine structure (EXAFS) spectra (in the 1−10 Å^{-1} range) for experimental samples against corresponding spectra from a library of reference standards. LCF was performed using Athena software.[38] The As reference standards included As(III)-sorbed ferrihydrite, As(V)-sorbed ferrihydrite, amorphous ferric arsenate (AFA), scorodite, and tooeleite.

Iron K-edge XAS spectra were collected at the Australian Synchrotron in transmission mode at room temperature using a Si(111) double crystal monochromator with an ionization chamber detector. The dried experimental samples were homogenized, pressed into pellets after dilution with cellulose,
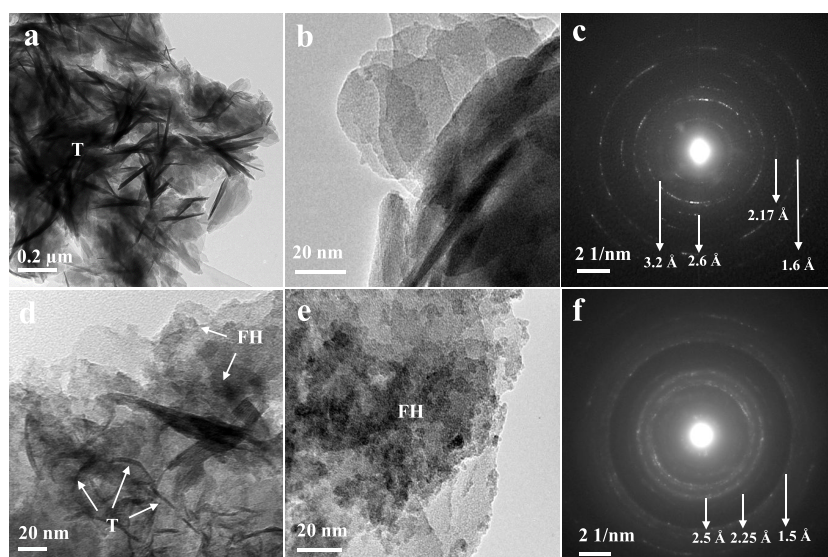
Figure 1. Bright field-TEM image of (a, b) initial tooeleite (T) and its (c) corresponding SAED pattern show four rings at 3.2, 2.6, 2.17, and 1.6 Å positions that are characteristic for tooeleite. (d, e) tooeleite and ferrihydrite (FH) aggregates observed in the 10 mM Fe(II) treatment under pH 8 conditions at a reaction time of 14 d and (f) the corresponding SAED pattern exhibit three diffuse rings at 2.5, 2.25, and 1.5 Å reflections.

and sealed with Kapton tape. Solid-phase Fe speciation was determined by the LCF analysis of the k^3-weighted EXAFS oscillations (in the 2−12 Å^{-1} range) of experimental samples against corresponding spectra from a library of reference standards including jarosite, lepidocrocite, green rust, ferrihydrite, goethite, and tooeleite. LCF of Fe K-edge EXAFS data over a k-range of up to 12 Å^{-1} has proven to be sufficient for differentiation among Fe(III) mineral phases in previous studies on the Fe(II)-induced transformation of Fe(III) oxides.[29]

RESULTS AND DISCUSSION

Characterization of the Initial Tooeleite. XRD confirmed that the mineral synthesis procedure produced tooeleite, with no other identifiable phases (Supporting Information Figure S1). The total As and Fe content in the synthesized tooeleite was 2.89 and 4.81 mmol g^{-1}, respectively, which equates to a molar As:Fe ratio of 0.60. This is comparable to the molar As:Fe ratio reported in natural tooeleite (e.g., Cesbron and Williams[20] found a ratio of 0.61) but is slightly lower than tooeleite's theoretically ideal stoichiometry (whereby As:Fe = 0.66). Arsenic K-edge XANES spectroscopy confirmed that the tooeleite-bound As was present as As(III) alone (Supporting Information Table S1). SEM with EDX showed that the synthesized tooeleite exhibited a platy aggregated structure and an As:Fe ratio of ~0.7 (Supporting Information Figure S2). TEM showed that the tooeleite was a multilayered nanocrystalline form with thick flake structures (Figure 1a,b). The TEM−selected area electron diffraction (SAED) pattern (Figure 1c) displays d-spacings of 3.2, 2.6, 2.17, and 1.6 Å that are equivalent with that of tooeleite.[18]

Solid-Phase Iron Speciation. Iron K-edge EXAFS spectroscopy indicates that negligible transformation of tooeleite occurred under Fe(II)-free conditions at pH 4 and 6, with only very minor transformation occurring over 14 days at pH 8 (Figure 2). Likewise, very little tooeleite transformation (amounting to only 6% of solid-phase Fe) occurred following the addition of 1 mM Fe(II) under pH 4 conditions.
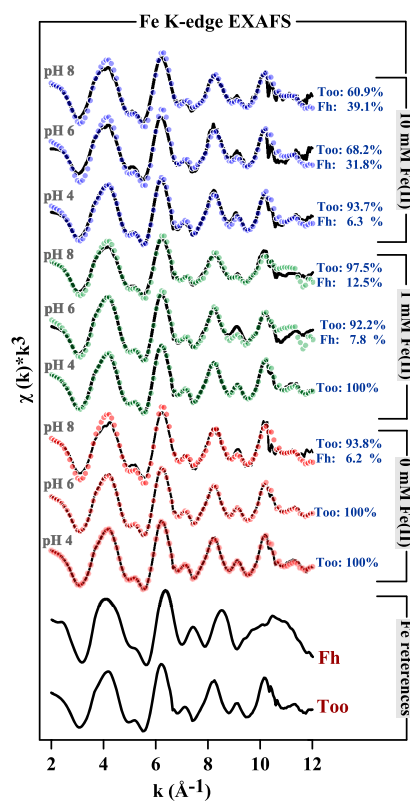
Figure 2. Iron K-edge EXAFS spectra of solid-phase material resulting from the exposure of tooeleite to 0, 1, and 10 mM Fe(II) at pH 4, 6, and 8 over 14 days, in comparison to reference spectra for tooeleite (Too) and ferrihydrite (Fh). Linear combination fits (colored circles) are superimposed on the experimental data (solid lines).

In contrast, the Fe K-edge EXAFS spectroscopic results show that substantial levels of tooeleite transformation occurred in response to the addition of Fe(II) at both pH 6 and 8. For example, at pH 8, 31 and 39% transformation of tooeleite-bound Fe(III) had occurred by day 14 following the addition of 10 mM Fe(II) (Figure 2).

LCF of the Fe K-edge EXAFS spectra indicates that Fe(II) induced the partial transformation of tooeleite-bound Fe(III) to a ferrihydrite-like Fe(III) species (Supporting Information Table S2). In agreement, TEM−SAED identified the presence of nanoscale ferrihydrite crystallites in the 10 mM Fe(II) treatment at pH 8 (Figure 1). In this case, the presence of ferrihydrite is evident from *d*-spacings at 2.50, 2.25, and 1.50 Å in the SAED pattern shown in Figure 1f. These *d*-spacings for ferrihydrite are readily distinguishable from those of tooeleite, which is further differentiated from ferrihydrite, given tooeleite's larger crystallite size and distinct morphology (Figure 1d). The newly formed ferrihydrite was X-ray amorphous, as no new XRD peaks (beyond those attributable to tooeleite) developed over the course of the experiment described here (Supporting Information Figure S3).

Solid-Phase Arsenic Speciation. LCF of As K-edge XANES spectra shows that As in all solid-phase samples collected over the 14-day experiment duration was present as As(III) (Figure 3a, Supporting Information Table S1). Arsenic
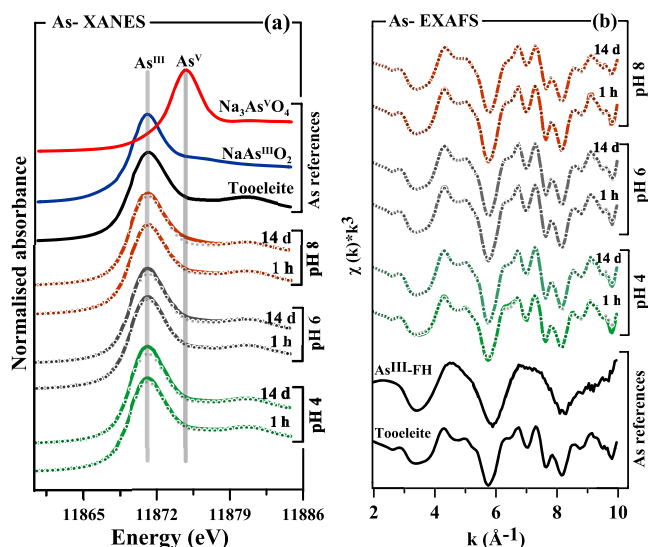
Figure 3. (a) Arsenic K-edge XANES spectra and (b) k^3 weighted EXAFS spectra of solid-phase materials collected after reaction with 10 mM Fe(II) for 1 h or 14 days at pH 4, 6, or 8. The vertical gray lines in panel (a) indicate the white line energy for As(III) and As(V). Solid and dotted lines represent experimental data and linear least-squares fits, respectively. As^{III}-FH denotes As(III) sorbed to ferrihydrite.

K-edge EXAFS spectroscopy shows that, in some treatments, tooeleite-bound As(III) transformed partially to As(III) sorbed to ferrihydrite (Figure 3b, Supporting Information Table S1). The extent of transformation of tooeleite-bound As(III) to ferrihydrite-sorbed As(III) varied as a function of both pH and the level of Fe(II) addition. In the absence of Fe(II), 0, 11 and 19% of tooeleite-bound As(III) had transformed to ferrihydrite-sorbed As(III) by day 14 at pH 4, 6, and 8, respectively (Supporting Information, Table S1).

In comparison to the Fe(II)-free treatments, much larger changes in solid-phase As speciation occurred in the 10 mM Fe(II) treatments. In these Fe(II)-rich treatments, ferrihydrite-sorbed As(III) comprised 10, 21, and 33% of solid-phase As under pH 4, 6, and 8 conditions, respectively, at day 14. Overall, the As and Fe K-edge EXAFS spectroscopy results show that the addition of Fe(II) under circumneutral pH conditions induced a significant transformation in solid-phase As speciation, whereby tooeleite-bound As(III) was partly replaced by As(III) sorbed to ferrihydrite (Figure 3).

In general, both the As and Fe K-edge EXAFS spectroscopy results point to Fe(II) acting to induce transformation of tooeleite to ferrihydrite at pH 6 and 8. From a quantitative perspective, the extent of transformation of tooeleite-bound As (up to 33% of solid-phase As) compares relatively well with the corresponding transformation of tooeleite-bound Fe (up to 39% of solid-phase). Although the percentage transformation of tooeleite-bound Fe does not exactly match transformation of tooeleite-bound As in each experiment treatment, the differences are in fact minor, considering that the accuracy of the LCF approach has been reported as approx. ±5%.[39]

Aqueous-Phase Arsenic Dynamics. Analysis of aqueous As speciation revealed the presence of As(III) alone, with no detectable As(V), in either control (Fe(II)-free) or Fe(II)-amended treatments over the 14 day experiment duration. As shown in Figure 4, mobilization of As(III) from the solid phase into the aqueous phase occurred (to varying degrees) in all experimental treatments. Both pH and the addition of Fe(II) had a significant effect on the magnitude of As(III) mobilization (Figure 4). Increases in pH (from 4 to 8) were found to enhance As(III) mobilization in the 0, 1, and 10 mM Fe(II) treatments. At pH 4, the presence of 1 or 10 mM Fe(II) had little effect (relative to the Fe(II)-free treatment) on the extent of As(III) mobilization from tooeleite.

In contrast, increasing the concentration of added Fe(II) (from 0 to 10 mM) at both pH 6 and 8 resulted in substantial
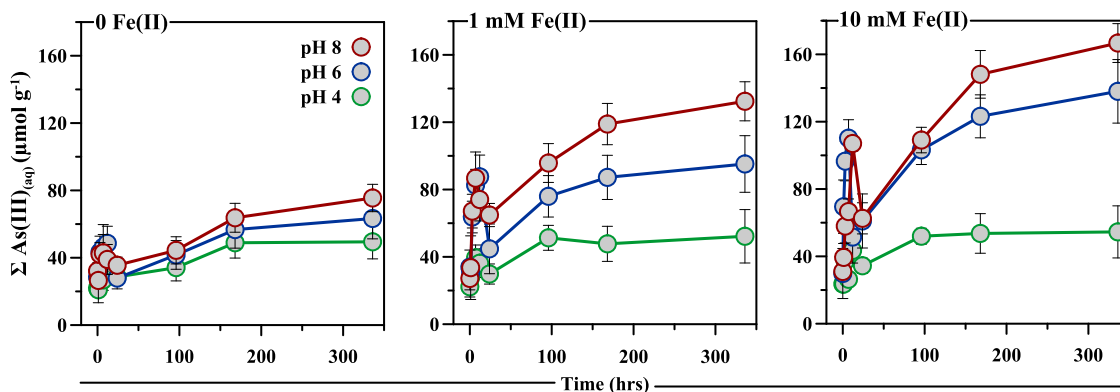
Figure 4. Temporal evolution of As(III)$_{(aq)}$ during the (a) 0 Fe(II), (b) 1 mM Fe(II), and (c) 10 mM Fe(II) induced reductive dissolution of tooeleite as a function of pH (4−8) over 14 days.

increases in As(III) mobilization. For example, at pH 8, the final amount of As(III) that was released to the aqueous phase following the addition of 10 mM Fe(II) was ~165 μmol g^{-1} compared to only ~75 μmol g^{-1} under Fe(II)-free conditions (Figure 4). This comparison indicates that the addition of 10 mM Fe(II) at pH 8 enhanced As(III) mobilization by more than twofold relative to the corresponding 0 mM Fe(II) treatment. On the whole, the results therefore show that the addition of Fe(II) under circumneutral pH conditions induced significant mobilization of As(III) into the aqueous phase (Figure 4), which occurred in parallel with Fe(II)-induced transformation of tooeleite to ferrihydrite (Figures 1 and 2).

Fe(II)-Induced Transformation of Tooeleite. The present study demonstrates, for the first time, that Fe(II) induces relatively rapid partial transformation of tooeleite under circumneutral pH conditions. As described previously for Fe(III) oxides,[29,20] the Fe(II)-induced transformation pathway is likely to occur via a cascade of processes involving (i) Fe(II) adsorption to the tooeleite surface, (ii) electron transfer between adsorbed Fe(II) and tooeleite-bound Fe(III), and (iii) conduction of transferred electrons to different Fe(III) lattice sites within tooeleite, which then (iv) undergo reductive release of Fe(II). During this Fe(II)/Fe(III) electron transfer−atom-exchange (ET-AE) process, Fe atoms are rapidly exchanged between the aqueous and solid phases, thereby accelerating the transformation of metastable Fe(III) phases to more stable phases.[29−32] The overall consequence of the ET-AE process is that tooeleite dissolves and As(III)-sorbed ferrihydrite precipitates, with this dissolution-precipitation transformation pathway occurring at rates that are accelerated under Fe(II)-rich conditions relative to Fe(II)-free conditions.

The initial requirement for Fe(II) sorption is consistent with our finding that the extent of Fe(II)-induced transformation of tooeleite increased from pH 6 and 8, but it was negligible at pH 4. In this regard, previous research demonstrates that Fe(II) adsorption to Fe(III) oxides is negligible under acidic conditions, and it increases significantly over a narrow pH range just below neutral pH. Strathmann and Stone,[40] for example, found that Fe(II) adsorption on hematite and goethite increased from negligible at pH < 5 to nearly 100% at pH > 7. A similar pH-dependent behavior has been reported by Burton et al.[41] for Fe(II) adsorption to schwertmannite. In this case, Fe(II)-induced transformation of schwertmannite was negligible at pH < 5 and was found to increase in line with the increased extent of Fe(II) adsorption at pH > 5.

A New Pathway for As(III) Mobilization. Our results show that the Fe(II)-induced transformation of tooeleite was associated with enhanced mobilization of As(III) into the aqueous phase. This is broadly consistent with the transformation of tooeleite to ferrihydrite (represented as Fe(OH)$_3$) according to the reaction

$$Fe_6(AsO_3)_4SO_4(OH)_4 \cdot 4H_2O_{(s)} + 8H_2O + 2OH^-$$
$$\rightarrow 6Fe(OH)_{3(s)} + 4H_3AsO_3^0 + SO_4^{2-}$$
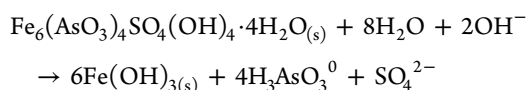
Although this equation points to the complete dissolution of all tooeleite-bound As(III), it is clear from our results that the ferrihydrite that forms via Fe(II)-induced transformation of tooeleite retains a large amount of the As(III) that was initially bound within tooeleite. This observation is consistent with previous work showing that ferrihydrite (or comparable phases, such "hydrous ferric oxide", HFO) can retain large amounts of

As(III). For example, Dixit and Hering[42] report a maximum sorption density for As(III) on HFO of 0.31 mol$_{As(III)}$ mol$_{Fe(III)}$$^{-1}$. Raven et al.[43] found an even higher maximum sorption density for As(III) on ferrihydrite of 0.60 mol$_{As(III)}$ mol$_{Fe(III)}$$^{-1}$.

Importantly, these previous reports suggest that ferrihydrite's ability to sorb As(III) is either less than or comparable to tooeleite's As(III) content (which is 0.66 mol$_{As(III)}$ mol$_{Fe(III)}$$^{-1}$ for tooeleite's ideal composition of Fe$_6$(AsO$_3$)$_4$SO$_4$(OH)$_4$· 4H$_2$O). Furthermore, the adsorption of large amounts of As(III) by ferrihydrite requires very high equilibrium aqueous As(III) concentrations. For example, Raven et al.[43] found that their maximum sorption density of 0.60 mol$_{As(III)}$ mol$_{Fe(III)}$$^{-1}$ for As(III) adsorption to ferrihydrite corresponded to an aqueous-phase concentration of ~15 mmol$_{As(III)}$ L^{-1} (at pH 4.6 and 9.2). This exceeds the As(III) concentration that results from equilibration of initially As-free solutions with tooeleite, which Zhu et al.[44] found from long-term (over 330 days) dissolution experiments to be within the range of 6−7 mmol$_{As(III)}$ L^{-1} (at pH 4−8). Overall, the quantitative comparisons discussed above support our observation that As(III) mobilization into the aqueous phase occurs during the transformation of tooeleite to ferrihydrite.

Our results show that ferrihydrite was the only detectable mineral produced via the Fe(II)-induced transformation of tooeleite. It would therefore appear that tooeleite is metastable with regard to ferrihydrite under the conditions examined in our experiment. However, it should be noted that ferrihydrite is itself metastable, readily undergoing rapid Fe(II)-induced transformation to more crystalline Fe(III) minerals such goethite, feroxyhyte, lepidocrocite, and magnetite.[31,34,45,46] In contrast to the expected role of Fe(II) in inducing ferrihydrite transformation, we found no evidence for the formation of these more crystalline products. Therefore, once formed, it appears that ferrihydrite persisted under the experimental conditions described here.

The persistence of ferrihydrite in the present study is consistent with high concentrations of sorbed As(III) acting to stabilize ferrihydrite against Fe(II)-induced transformation. This effect of As(III) has been reported previously from studies into the Fe(II)-induced transformation of both ferrihydrite and schwertmannite.[33,35] In this case, ferrihydrite stabilization may result from surface-complexed As(III) passivating the mineral surface against Fe(II) adsorption and/or interfering with electron transfer processes following the adsorption of Fe(II).

Environmental Implications. Tooeleite forms from As(III)- and Fe(III)-rich solutions at low pH and is relatively stable under oxidizing conditions at pH 2−3.5.[19] Although tooeleite appears to persist under low pH conditions, previous work has indicated that tooeleite becomes unstable at pH > 3.5, Opio[47] conducted long-term stability tests (over 30 weeks) showing that tooeleite gradually transformed at pH 4−9 to form a poorly ordered "ferric arsenite" phase. Likewise, Chai et al.[48] found that tooeleite transformed at pH 6 and 9 to an "amorphous ferric compound" with broad XRD peaks similar to those of 2-line ferrihydrite.

Previous studies on tooeleite stability at pH > 3.5 have considered oxic conditions where Fe(II) is absent.[25,26,47,48] The present study is significant in that it is the first to evaluate tooeleite stability under anoxic conditions at higher pH. Under such conditions, Fe(II) can be produced by microbially mediated Fe(III) reduction and may subsequently interact

with tooeleite. Higher pH conditions (relative to the initially acidic conditions under which tooeleite forms) can be driven by microbial Fe(III) reduction coupled to the oxidation of organic C.[6,41] Higher pH can also develop via neutralization of acidic tooeleite-bearing mine waste or mine-site soil by (i) deliberate addition of acid-consuming material (e.g., lime) as a management strategy, or (ii) the natural presence of slowly-reactive acid-neutralizing minerals whereby in-situ neutralization lags behind rapid initial acid generation.

The results from the present study show, for the first time, that Fe(II) induces transformation of tooeleite under anoxic, circumneutral pH conditions. The Fe(II)-induced transformation of tooeleite results in formation of ferrihydrite, which appears to be stabilized by large amounts of sorbed As(III). It also results in mobilization of elevated concentrations of As(III) into the aqueous phase. This finding highlights a novel pathway for As(III) mobilization in tooeleite-bearing systems, and challenges the concept that tooeleite represents a stable host phase for minimizing As(III) mobility.

The findings from this study have important implications for situations where tooeleite-bearing mine wastes, mine-site soils and other materials may be exposed to waterlogged, circumneutral conditions. It is likely that, under such conditions, tooeleite will experience rapid Fe(II)-induced transformation causing it to become a source for release of As(III) into ground- and surface-waters. This work deepens our understanding of how Fe cycling and associated mineralogical transformations can influence As mobility and fate in mining-impacted systems.

ASSOCIATED CONTENT

Ⓢ Supporting Information

The Supporting Information is available free of charge at https://pubs.acs.org/doi/10.1021/acs.est.2c02130.

Characterization of initial tooeleite and its transformation products (Figures S1–S3), and temporal changes of solid-phase arsenic and iron speciation (Tables S1 and S2) (PDF)

AUTHOR INFORMATION

Corresponding Author

Girish Choppala − Global Centre for Environmental Remediation (GCER), The University of Newcastle, Callaghan, New South Wales 2308, Australia; ◉ orcid.org/0000-0002-8866-5001; Phone: +61 240553191; Email: girish.choppala@newcastle.edu.au

Authors

Dane Lamb − Chemical and Environmental Engineering, School of Engineering, RMIT University, Melbourne, Victoria 3000, Australia; ◉ orcid.org/0000-0003-2303-5460

Robert Aughterson − Institute of Materials Engineering, Australian Nuclear Science and Technology Organization (ANSTO), Sydney, New South Wales 2234, Australia

Edward D. Burton − Faculty of Science and Engineering, Southern Cross University, Lismore, New South Wales 2480, Australia; ◉ orcid.org/0000-0002-9628-089X

Complete contact information is available at:
https://pubs.acs.org/10.1021/acs.est.2c02130

REFERENCES

(1) O'Day, P. A. Chemistry and Mineralogy of Arsenic. Elements 2006, 2, 77−83.

(2) Morin, G.; Calas, G. Arsenic in Soils, Mine Tailings, and Former Industrial Sites. Elements 2006, 2, 97−101.

(3) Berg, M.; Tran, H. C.; Nguyen, T. C.; Pham, H. V.; Schertenleib, R.; Giger, W. Arsenic Contamination of Groundwater and Drinking Water in Vietnam: A Human Health Threat. Environ. Sci. Technol. 2001, 35, 2621−2626.

(4) Rodríguez-Lado, L.; Sun, G.; Berg, M.; Zhang, Q.; Xue, H.; Zheng, Q.; Johnson, C. A. Groundwater Arsenic Contamination Throughout China. Science 2013, 341, 866.

(5) Van Den Berghe, M. D.; Jamieson, H. E.; Palmer, M. J. Arsenic mobility and characterization in lakes impacted by gold ore roasting, Yellowknife, NWT, Canada. Environ. Pollut. 2018, 234, 630−641.

(6) Burton, E. D.; Karimian, N.; Johnston, S. G.; Schoepfer, V. A.; Choppala, G.; Lamb, D. Arsenic-Imposed Effects on Schwertmannite and Jarosite Formation in Acid Mine Drainage and Coupled Impacts on Arsenic Mobility. ACS Earth Space Chem. 2021, 5, 1418−1435.

(7) Lamb, D.; Sanderson, P.; Wang, L.; Kader, M.; Naidu, R., Phytocapping of Mine Waste at Derelict Mine Sites in New South Wales. In Spoil to Soil: Mine Site Rehabilitation and Revegetation, 2017; 215−239.

(8) Ashley, P. M.; Lottermoser, B. G. Arsenic contamination at the Mole River mine, northern New South Wales. Aust. J. Earth Sci. 1999, 46, 861−874.

(9) Abraham, J.; Dowling, K.; Florentine, S. Assessment of potentially toxic metal contamination in the soils of a legacy mine site in Central Victoria, Australia. Chemosphere 2018, 192, 122−132.

(10) Johnston, S. G.; Bennett, W. W.; Doriean, N.; Hockmann, K.; Karimian, N.; Burton, E. D. Antimony and arsenic speciation, redox-cycling and contrasting mobility in a mining-impacted river system. Sci. Total Environ. 2020, 710, No. 136354.

(11) Bowell, R. J.; Alpers, C. N.; Jamieson, H. E.; Nordstrom, D. K.; Majzlan, J. The Environmental Geochemistry of Arsenic — An Overview. Rev. Mineral. Geochem. 2014, 79, 1−16.

(12) Drahota, P.; Rohovec, J.; Filippi, M.; Mihaljevič, M.; Rychlovský, P.; Červený, V.; Pertold, Z. Mineralogical and geochemical controls of arsenic speciation and mobility under different redox conditions in soil, sediment and water at the Mokrsko-West gold deposit, Czech Republic. Sci. Total Environ. 2009, 407, 3372−3384.

(13) Campbell, K. M.; Nordstrom, D. K. Arsenic Speciation and Sorption in Natural Environments. *Rev. Mineral. Geochem.* **2014**, *79*, 185−216.

(14) Ona-Nguema, G.; Morin, G.; Juillot, F.; Calas, G.; Brown, G. E. EXAFS Analysis of Arsenite Adsorption onto Two-Line Ferrihydrite, Hematite, Goethite, and Lepidocrocite. *Environ. Sci. Technol.* **2005**, *39*, 9147−9155.

(15) Majzlan, J.; Drahota, P.; Filippi, M. Parageneses and crystal chemistry of arsenic minerals. *Rev. Mineral. Geochem.* **2014**, *79*, 17−184.

(16) Morin, G.; Juillot, F.; Casiot, C.; Bruneel, O.; Personné, J.-C.; Elbaz-Poulichet, F.; Leblanc, M.; Ildefonse, P.; Calas, G. Bacterial Formation of Tooeleite and Mixed Arsenic(III) or Arsenic(V)−Iron(III) Gels in the Carnoulès Acid Mine Drainage, France. A XANES, XRD, and SEM Study. *Environ. Sci. Technol.* **2003**, *37*, 1705−1712.

(17) Egal, M.; Casiot, C.; Morin, G.; Parmentier, M.; Bruneel, O.; Lebrun, S.; Elbaz-Poulichet, F. Kinetic control on the formation of tooeleite, schwertmannite and jarosite by Acidithiobacillus ferrooxidans strains in an As(III)-rich acid mine water. *Chem. Geol.* **2009**, *265*, 432−441.

(18) Morin, G.; Rousse, G.; Elkaim, E. Crystal structure of tooeleite, Fe6(AsO3)4SO4(OH)4·4H2O, a new iron arsenite oxyhydroxysulfate mineral relevant to acid mine drainage. *Am. Mineral.* **2007**, *92*, 193−197.

(19) Nishimura, T.; Robins, R. G. Confirmation that tooeleite is a ferric arsenite sulfate hydrate, and is relevant to arsenic stabilization. *Miner. Eng.* **2008**, *21*, 246−251.

(20) Cesbron, F. P.; Williams, S. A. Tooeleite, a new mineral from the U.S. Mine, Tooele County, Utah. *Mineral. Mag.* **1992**, *56*, 71−73.

(21) Márquez, M.; Gaspar, J.; Bessler, K. E.; Magela, G. Process mineralogy of bacterial oxidized gold ore in São Bento Mine (Brasil). *Hydrometallurgy* **2006**, *83*, 114−123.

(22) Meunier, L.; Walker, S. R.; Wragg, J.; Parsons, M. B.; Koch, I.; Jamieson, H. E.; Reimer, K. J. Effects of Soil Composition and Mineralogy on the Bioaccessibility of Arsenic from Tailings and Soil in Gold Mine Districts of Nova Scotia. *Environ. Sci. Technol.* **2010**, *44*, 2667−2674.

(23) DeSisto, S. L.; Jamieson, H. E.; Parsons, M. B. Subsurface variations in arsenic mineralogy and geochemistry following long-term weathering of gold mine tailings. *Appl. Geochem.* **2016**, *73*, 81−97.

(24) Fazle Bari, A. S. M.; Lamb, D.; Choppala, G.; Bolan, N.; Seshadri, B.; Rahman, M. A.; Rahman, M. M. Geochemical fractionation and mineralogy of metal(loid)s in abandoned mine soils: Insights into arsenic behaviour and implications to remediation. *J. Hazard. Mater.* **2020**, *399*, No. 123029.

(25) Liu, J.; He, L.; Chen, S.; Dong, F.; Frost, R. L. Characterization of the dissolution of tooeleite under Acidithiobacillus ferrooxidans relevant to mineral trap for arsenic removal. *Desalin. Water Treat.* **2016**, *57*, 15108−15114.

(26) Chai, L.; Yue, M.; Li, Q.; Zhang, G.; Zhang, M.; Wang, Q.; Liu, H.; Liu, Q. Enhanced stability of tooeleite by hydrothermal method for the fixation of arsenite. *Hydrometallurgy* **2018**, *175*, 93−101.

(27) Troyer, L. D.; Stone, J. J.; Borch, T. Effect of biogeochemical redox processes on the fate and transport of As and U at an abandoned uranium mine site: an X-ray absorption spectroscopy study. *Environ. Chem.* **2014**, *11*, 18−27.

(28) Burton, E. D.; Hockmann, K.; Karimian, N. Antimony Sorption to Goethite: Effects of Fe(II)-Catalyzed Recrystallization. *ACS Earth Space Chem.* **2020**, *4*, 476−487.

(29) Boland, D. D.; Collins, R. N.; Miller, C. J.; Glover, C. J.; Waite, T. D. Effect of Solution and Solid-Phase Conditions on the Fe(II)-Accelerated Transformation of Ferrihydrite to Lepidocrocite and Goethite. *Environ. Sci. Technol.* **2014**, *48*, 5477−5485.

(30) Choppala, G.; Burton, E. D. Chromium(III) substitution inhibits the Fe(II)-accelerated transformation of schwertmannite. *PLoS One* **2018**, *13*, No. e0208355.

(31) Hansel, C. M.; Benner, S. G.; Fendorf, S. Competing Fe(II)-Induced Mineralization Pathways of Ferrihydrite. *Environ. Sci. Technol.* **2005**, *39*, 7147−7153.

(32) Karimian, N.; Johnston, S. G.; Burton, E. D. Antimony and Arsenic Behavior during Fe(II)-Induced Transformation of Jarosite. *Environ. Sci. Technol.* **2017**, *51*, 4259−4268.

(33) Zhang, G.; Yuan, Z.; Lei, L.; Lin, J.; Wang, X.; Wang, S.; Jia, Y. Arsenic redistribution and transformation during Fe(II)-catalyzed recrystallization of As-adsorbed ferrihydrite under anaerobic conditions. *Chem. Geol.* **2019**, *525*, 380−389.

(34) ThomasArrigo, L. K.; Mikutta, C.; Byrne, J.; Kappler, A.; Kretzschmar, R. Iron(II)-Catalyzed Iron Atom Exchange and Mineralogical Changes in Iron-rich Organic Freshwater Flocs: An Iron Isotope Tracer Study. *Environ. Sci. Technol.* **2017**, *51*, 6897−6907.

(35) Burton, E. D.; Johnston, S. G.; Watling, K.; Bush, R. T.; Keene, A. F.; Sullivan, L. A. Arsenic Effects and Behavior in Association with the Fe(II)-Catalyzed Transformation of Schwertmannite. *Environ. Sci. Technol.* **2010**, *44*, 2016−2021.

(36) Li, X.; Zhao, F.; Deng, S. The removal of Arsenic (III) from acid mine drainage by mineral trap of tooeleite (Fe6 (AsO3) 4SO4 (OH) 4· 4H2O). *An Interdisciplinary Response to Mine Water Challenges* **2014**, 671−674.

(37) Chen, Z.; Akter, K. F.; Rahman, M. M.; Naidu, R. The separation of arsenic species in soils and plant tissues by anion-exchange chromatography with inductively coupled mass spectrometry using various mobile phases. *Microchem. J.* **2008**, *89*, 20−28.

(38) Ravel, B.; Newville, M. ATHENA, ARTEMIS, HEPHAESTUS: data analysis for X-ray absorption spectroscopy using IFEFFIT. *J. Synchrotron Radiat.* **2005**, *12*, 537−541.

(39) Bostick, B. C.; Chen, C.; Fendorf, S. Arsenite Retention Mechanisms within Estuarine Sediments of Pescadero, CA. *Environ. Sci. Technol.* **2004**, *38*, 3299−3304.

(40) Strathmann, T. J.; Stone, A. T. Mineral surface catalysis of reactions between FeII and oxime carbamate pesticides. *Geochim. Cosmochim. Acta* **2003**, *67*, 2775−2791.

(41) Burton, E. D.; Bush, R. T.; Sullivan, L. A.; Mitchell, D. R. G. Schwertmannite transformation to goethite via the Fe(II) pathway: Reaction rates and implications for iron-sulfide formation. *Geochim. Cosmochim. Acta* **2008**, *72*, 4551−4564.

(42) Dixit, S.; Hering, J. G. Comparison of arsenic(V) and arsenic(III) sorption onto iron oxide minerals: Implications for arsenic mobility. *Environ. Sci. Technol.* **2003**, *37*, 4182−4189.

(43) Raven, K.; Jain, A.; Loeppert, R. H. Arsenite and arsenate adsorption on ferrihydrite: Kinetics, equilibrium, and adsorption envelopes. *Environ. Sci. Technol.* **1998**, *32*, 344−349.

(44) Zhu, Z.; Zhang, J.; Zhu, Y.; Liu, J.; Tang, S.; Zhang, L.; Wang, Y. Dissolution, stability and solubility of tooeleite [Fe6(AsO3)4-(SO4)(OH)4·4H2O] at 25−45°C and pH 2−12. *Minerals* **2020**, *10*, 921.

(45) Burton, E. D.; Hockmann, K.; Karimian, N.; Johnston, S. G. Antimony mobility in reducing environments: The effect of microbial iron(III)-reduction and associated secondary mineralization. *Geochim. Cosmochim. Acta* **2019**, *245*, 278−289.

(46) Hockmann, K.; Karimian, N.; Schlagenhauff, S.; Planer-Friedrich, B.; Burton, E. D. Impact of Antimony(V) on Iron(II)-Catalyzed Ferrihydrite Transformation Pathways: A Novel Mineral Switch for Feroxyhyte Formation. *Environ. Sci. Technol.* **2021**, *55*, 4954−4963.

(47) Opio, F. K., *Investigation of Fe (III)-As (III) bearing phases and their potential for arsenic disposal*; Queen's University (Canada): 2013.

(48) Chai, L.; Yue, M.; Yang, J.; Wang, Q.; Li, Q.; Liu, H. Formation of tooeleite and the role of direct removal of As(III) from high-arsenic acid wastewater. *J. Hazard. Mater.* **2016**, *320*, 620−627.